Inorg. Chem. **2008**, *47*, 1391−1396

Subtle Ring-Constraint Effects on the Formation of Metallacycles. Cyclodimer versus Cyclotrimer of Bis(chloro)-1,4-bis(dimethyl-3 or 4-pyridylsilyl)benzenepalladium(II) Complexes

Young Mee Na,[†] Tae Hwan Noh,[†] In Sung Chun,[†] Young-A Lee,[‡] Jongki Hong,[§] and Ok-Sang Jung*[,†]

Department of Chemistry and Center for Plastic Information Systems, Pusan National University, Pusan 609-735, Korea, Department of Chemistry, Chonbuk National University, Jeonju 561-756, Korea, and College of Pharmacy, Kyung Hee University, Seoul 130-701, Korea

Received July 26, 2007

Stepwise modulation of the ring size of metallacyclic compounds via subtle ring-constraint effects has been established. The reactions of (COD)$PdCl_2$ with *p*- or *m*-psb ligand [COD = 1,5-cyclooctadiene; *p*-psb = 1,4-bis(dimethyl-4-pyridylsilyl)benzene; *m*-psb = 1,4-bis(dimethyl-3-pyridylsilyl)benzene] in a mixture of acetone and ethanol at room temperature produce the metallacyclodimers $[PdCl_2(p\text{- or } m\text{-psb})]_2$. The cyclodimeric species of $[PdCl_2(p\text{-psb})]_2$ at the boiling temperature or via the sonication of the chloroform solution is completely converted to the cyclotrimer $[PdCl_2(p\text{-psb})]_3$. Direct reaction of (COD)$PdCl_2$ with *p*-psb in a mixture of acetone and ethanol at reflux temperature yields the same trimer, $[PdCl_2(p\text{-psb})]_3$. Furthermore, equilibria between the kinetic product, $[PdCl_2(p\text{-psb})]_2$, and the thermodynamic product, $[PdCl_2(p\text{-psb})]_3$, have been observed in *N*,*N*-dimethylformamide as well as in dimethyl sulfoxide. In contrast, the cyclodimeric structure of $[PdCl_2(m\text{-psb})]_2$ is retained under the same treatment conditions for 40 h; that is, the trimeric species, $[PdCl_2(m\text{-psb})]_3$, is not formed. Such a notable difference between $[PdCl_2(p\text{-psb})]_2$ and $[PdCl_2(m\text{-psb})]_2$ might be explained by their different angle constraints.

Introduction

The ability to control macrocyclic rings by means of chemical triggers is of importance in the construction of molecular machines and switches as well as in aesthetic appeal.[1–5] In particular, various metallamacrocyclic complexes have been studied for their important building blocks in the construction of functional supramolecular materials that can be utilized for molecular recognition, selective transformation, drug-delivery systems, catalysts, storage, and biomimics.[6–15] One of facile synthetic methods is ring expansion,[16–18] including cavity control[19,20] by means of labile metal–ligand coordination and thermodynamic control. Among the various metallacycles, palladium(II) complexes of multidentate nitrogen-donor ligands have contributed to the synthesis of unique metal coordination materials such

* To whom correspondence should be addressed. E-mail: oksjung@pusan.ac.kr.
[†] Pusan National University.
[‡] Chonbuk National University.
[§] Kyung Hee University.

(1) Stang, P. J.; Olenyuk, B. *Acc. Chem. Res.* **1997**, *30*, 502.
(2) Beissel, T.; Powers, R. E.; Raymond, K. N. *Angew. Chem., Int. Ed. Engl.* **1996**, *35*, 1084.
(3) Balladini, R.; Balzani, V.; Credi, A.; Gandolfi, M. T.; Venturi, M. *Acc. Chem. Res.* **2001**, *34*, 445.
(4) Davis, A. V.; Yeh, R. M.; Raymond, K. M. *Proc. Natl. Acad. Sci.* **2002**, *99*, 4793.
(5) Lehn, J.-M. *Supramolecular Chemistry: Concepts and Perspectives*; VCH: Weinheim, Germany, 1995.
(6) Swiegers, G. F.; Malefetse, T. J. *Coord. Chem. Rev.* **2002**, *225*, 91.
(7) Cotton, F. A.; Lin, C.; Murillo, C. A. *Acc. Chem. Res.* **2001**, *34*, 759.
(8) Leinigner, S.; Olenyuk, B.; Stang, P. J. *Chem. Rev.* **2000**, *100*, 853–7.
(9) Jude, H.; Disteldorf, H.; Fischer, S.; Wedge, T.; Hawkridge, A. M.; Arif, A. M.; Hawthorne, M. F.; Muddiman, D. C.; Stang, P. J. *J. Am. Chem. Soc.* **2005**, *127*, 12131.
(10) Wang, P.; Moorefield, C. N.; Newkome, G. R. *Angew. Chem., Int. Ed.* **2005**, *44*, 1679.
(11) Grote, Z.; Scopelliti, R.; Severin, K. *J. Am. Chem. Soc.* **2004**, *126*, 16959.
(12) Benkstein, K. D.; Hupp, J. T.; Stern, C. L. *J. Am. Chem. Soc.* **1998**, *120*, 12982.
(13) Jung, O.-S.; Lee, Y.-A.; Kim, Y. J.; Hong, J. *Cryst. Growth Des.* **2002**, *2*, 497.
(14) Uehara, K.; Kasai, K.; Mizuno, N. *Inorg. Chem.* **2007**, *46*, 2563.
(15) Zhang, Z.; Cai, R.; Chen, Z.; Zhou, X. *Inorg. Chem.* **2007**, *46*, 321.
(16) Fujita, M.; Tominaga, M.; Hori, A.; Therrien, B. *Acc. Chem. Res.* **2005**, *38*, 369.
(17) Habermehl, N. C.; Eisler, D. J.; Kirby, C. W.; Yue, N. L.-S.; Puddephatt, R. J. *Organometallics* **2006**, *25*, 2921.
(18) Fujita, M. *Chem. Soc. Rev.* **1998**, *27*, 417.
(19) Farrell, J. R.; Mirkin, C. A.; Guzei, I. A.; Liable-Sands, L. M.; Rheingold, A. L. *Angew. Chem., Int. Ed.* **1998**, *37*, 465.
(20) Gianneschi, N. C.; Masar, M. S., III; Mirkin, C. A. *Acc. Chem. Res.* **2005**, *38*, 825.

10.1021/ic701489p CCC: $40.75
Published on Web 01/12/2008

as catalysts,[21] rectangle building blocks,[22] submicrospheres,[23] task-specific morphology,[24] and a "magic ring" with an associative/dissociative dual-character Pd−N bond.[25] Of the nitrogen-donor ligands, silicon-containing pyridyl ligands have been found to be useful for the synthesis of desirable skeletal structures because they are adjustable in bridging ability and length, possess flexible angles around silicon, and are conformationally nonrigid.[26–30] Equilibria of ionic metallacyclic compounds containing NO_3^-, PF_6^-, or OTf^- have been observed,[31,32] but similar research on neutral metal complexes is very rare. In this context, control of the ring size of neutral metallamacrocyclic compounds remains unexplored.

In this paper, we report the stepwise ring expansion and equilibrium of a new metallamacrocyclic architecture based on the reaction of a square-planar unit, $(COD)PdCl_2$ with 1,4-bis(dimethyl-3 or 4-pyridylsilyl)benzene (*m*- or *p*-psb), according to a unique horse-shoe motif. This is the first report demonstrating the complete stepwise ring expansion of metallamacrocycles via subtle ring-constraint effects.

Experimental Section

Materials and Measurements. Palladium(II) chloride, 1,5-cyclooctadiene (COD), and 1,4-bis(chlorodimethylsilyl)benzene were purchased from Aldrich and used without further purification. $(COD)PdCl_2$ was prepared according to the procedure described in the literature.[33] 1,4-Bis(dimethyl-4-pyridylsilyl)benzene (*p*-psb) and 1,4-bis(dimethyl-3-pyridylsilyl)benzene (*m*-psb) were prepared by the method outlined in two of our previous reports.[34,35] ^{1}H NMR spectra were recorded on a Varian Gemini 300 operating at 300.00 MHz, and the chemical shifts were relative to the internal Me_4Si. IR spectra were obtained on a Perkin-Elmer 16F PC FTIR spectrophotometer with samples prepared as KBr pellets. Elemental microanalyses (C, H, and N) were performed on solid samples by the Advanced Analytical Division at KBSI, using a Perkin-Elmer 2400 CHNS analyzer. Thermal analyses were performed under a nitrogen atmosphere at a scan rate of 10 °C/min with a Stanton Red Croft TG 100. Sonication was carried out using a Branson Ultrasonic 2510R-DTH. Mass spectrometric (MS) analysis via a fast atom bombardment technique was performed in chloroform using a KMS-700 Mstation mass spectrometer (Jeol, Japan) and an MS-MP9020D data system.

$[PdCl_2(p\text{-psb})]_2$. An acetone solution (7.5 mL) of *p*-psb (3.5 mg, 0.01 mmol) was slowly diffused into an ethanol solution (7.5 mL) of $(COD)PdCl_2$ (2.9 mg, 0.01 mmol) in a Pyrex glass vial. Yellow crystals of $[PdCl_2(p\text{-psb})]_2$, suitable for X-ray crystallographic characterization, formed at the interface and were obtained in 63% yield after 7 days. Elemental analysis was carried out after evaporation of solvate ethanol molecules in vacuo. Anal. Calcd for $C_{40}H_{48}Cl_4N_4Pd_2Si_4$: C, 45.68; H, 4.60; N, 5.33. Found: C, 45.68; H, 4.66; N, 5.30. IR (KBr, cm^{-1}): 3060(w), 2954(w), 1603(w), 1415(m), 1254(m), 1132(s), 806(s), 779(s), 654(w), 521(m). ^{1}H NMR ($CDCl_3$, $SiMe_4$, ppm): δ 0.63 (s, 24H), 7.19 (d, $J = 6.3$ Hz, 8H), 7.50 (s, 8H), 8.64 (d, $J = 6.3$ Hz, 8H). MS: *m/e* 1017.6 $[M - Cl]^+$ (calcd *m/e* 1017.0).

$[PdCl_2(m\text{-psb})]_2$. An acetone solution (7.5 mL) of *m*-psb (3.5 mg, 0.01 mmol) was slowly diffused into an ethanol solution (7.5 mL) of $(COD)PdCl_2$ (2.9 mg, 0.01 mmol) in a Pyrex glass vial. Yellow crystals of $[PdCl_2(m\text{-psb})]_2$, suitable for X-ray crystallographic characterization, formed at the interface and were obtained in 68% yield after 4 days. Anal. Calcd for $C_{40}H_{48}Cl_4N_4Pd_2Si_4$: C, 45.68; H, 4.60; N, 5.33. Found: C, 45.60; H, 4.62; N, 5.30. IR (KBr, cm^{-1}): 3040(w), 2954(w), 1591(m), 1402(m), 1252(m), 1135(s), 814(s), 775(s), 694(m), 515(m), 485(m). ^{1}H NMR ($CDCl_3$, $SiMe_4$, ppm): 0.59 (s, 24H), 7.31 (t, $J = 6.6$ Hz, 4H), 7.49 (s, 8H), 7.90 (d, $J = 7.2$ Hz, 4H), 8.78 (d, $J = 5.7$ Hz, 4H), 8.83 (s, 4H). MS: *m/e* 1017.6 $[M - Cl]^+$ (calcd *m/e* 1017.0).

$[PdCl_2(p\text{-psb})]_3$. *Method 1*: A chloroform solution (5 mL) of $[PdCl_2(p\text{-psb})]_2$ (5.2 mg, 0.005 mmol) was sonicated for 40 h. *Method 2*: A chloroform solution (5 mL) of $[PdCl_2(p\text{-psb})]_2$ (5.2 mg, 0.005 mmol) was refluxed for 12 h. *Method 3*: Direct reaction of $(COD)PdCl_2$ (8.7 mg, 0.03 mmol) in ethanol (15 mL) with *p*-psb (10.5 mg, 0.03 mmol) in acetone (15 mL) was accomplished at reflux temperature for 24 h. Then, the solvent was evaporated to dryness to yield a thin yellow solid. The crude product was recrystallized in a mixture of chloroform and nitromethane but resulted in highly chloroform-solvated crystals (Supporting Information) unsuitable for X-ray crystallography. Thus, after the solvate molecules were completely evaporated, elemental analysis (C, H, and N) of the product was accomplished. Anal. Calcd for $C_{60}H_{72}Cl_6N_6Pd_3Si_6$: C, 45.68; H, 4.60; N, 5.33. Found: C, 45.50; H, 4.58; N, 5.34. IR (KBr, cm^{-1}): 3040(w), 2952(w), 1603(m), 1414(s), 1252(m), 1132(s), 800(s), 775(s), 669(m), 490(m). ^{1}H NMR ($CDCl_3$, $SiMe_4$, ppm): δ 0.57 (s, 36H), 7.37 (d, $J = 6.3$ Hz, 12H), 7.46 (s, 12H), 8.71 (d, $J = 6.3$ Hz, 12H). MS: *m/e* 1541.4 $[M - Cl]^+$ (calcd *m/e* 1541), 1193.6 $[M - Cl - L]^+$ (calcd *m/e* 1193), 1157.7 $[M - L - Cl - HCl]^+$ (calcd *m/e* 1157), 1018.0 $[M - PdCl_2 - L - Cl]^+$ (calcd *m/e* 1018.0).

Crystal Structure Determination. X-ray data were collected on a Bruker SMART automatic diffractometer with graphite-monochromated Mo Kα radiation ($\lambda = 0.710\,73$ Å) and a CCD detector at ambient temperature. A total of 45 frames of two-dimensional diffraction images were collected and processed to obtain the cell parameters and orientation matrix. The data were corrected for Lorentz and polarization effects. The absorption effects were corrected using the empirical ψ-scan method. The structures were solved using direct methods (*SHELXS 97*) and refined by full-matrix least-squares techniques (*SHELXL 97*).[36] The non-hydrogen atoms were refined anisotropically, and the hydrogen atoms were placed in calculated positions and refined only for the isotropic

(21) Yao, Q.; Kinney, E. P.; Zheng, C. *Org. Lett.* **2004**, *6*, 2997.
(22) Fujita, M.; Ibukuro, F.; Hagihara, H.; Ogura, K. *Nature* **1994**, *367*, 720.
(23) Chun, I. S.; Lee, K. S.; Hong, J.; Do, Y.; Jung, O.-S. *Chem. Lett.* **2007**, 548.
(24) Chun, I. S.; Kwon, J. A.; Yoon, H. J.; Bae, M. N.; Hong, J.; Jung, O.-S. *Angew. Chem., Int. Ed.* **2007**, *46*, 4960.
(25) Seidel, S. R.; Stang, P. J. *Acc. Chem. Res.* **2002**, *35*, 972.
(26) Jung, O.-S.; Kim, Y. J.; Kim, K. M.; Lee, Y.-A. *J. Am. Chem. Soc.* **2002**, *124*, 7906.
(27) Jung, O.-S.; Lee, Y.-A.; Kim, Y. J. *Chem. Lett.* **2002**, 1906.
(28) Jung, O.-S.; Kim, Y. J.; Lee, Y.-A.; Kang, S. W.; Choi, S. N. *Cryst. Growth Des.* **2004**, *4*, 23.
(29) Lee, J. W.; Kim, E. A.; Kim, Y. J.; Lee, Y.-A.; Pak, Y.; Jung, O.-S. *Inorg. Chem.* **2005**, *44*, 3151.
(30) Schmitz, M.; Leninger, S.; Fan, J.; Arif, A. M.; Stang, P. J. *Organometallics* **1999**, *18*, 4817.
(31) Fujita, M.; Sasaki, O.; Mitsuhashi, T.; Fujita, T.; Yajaki, J.; Yamaguchi, K.; Ogura, K. *Chem. Commun.* **1996**, 1353.
(32) Chun, I. S.; Moon, S. J.; Na, Y. M.; Lee, Y.-A.; Yoo, K. H.; Jung, O.-S. *Inorg. Chem. Commun.* **2007**, *10*, 967.
(33) Kharasch, M. S.; Seyler, R. C.; Mayo, F. R. *J. Am. Chem. Soc.* **1938**, *60*, 882.
(34) Park, B. I.; Chun, I. S.; Lee, Y.-A.; Park, K.-M.; Jung, O.-S. *Inorg. Chem.* **2006**, *45*, 4310.
(35) Cha, M. S.; Park, B. I.; Kang, H. J.; Yoo, K. H.; Jung, O.-S. *Bull. Korean Chem. Soc.* **2007**, *28*, 1057.
(36) Sheldrick G. M. *SHELXS-97: A Program for Structure Determination*; University of Göttingen: Göttingen, Germany, 1997.

Table 1. Crystallographic Data for $[PdCl_2(p\text{-psb})]_2$ and $[PdCl_2(m\text{-psb})]_2$

	$[PdCl_2(p\text{-psb})]_2$	$[PdCl_2(m\text{-psb})]_2$
formula	$C_{40}H_{48}N_4Cl_4Si_4Pd_2 \cdot (C_2H_5OH)$	$C_{40}H_{48}N_4Cl_4Si_4Pd_2$
M_w	1143.92	1051.78
cryst syst	triclinic	triclinic
space group	$P\bar{1}$	$P\bar{1}$
a/Å	8.4631(5)	8.5122(6)
b/Å	12.2210(8)	10.8590(7)
c/Å	13.8289(9)	13.3190(9)
α/deg	83.164(1)	78.353(1)
β/deg	72.731(1)	81.993(1)
γ/deg	82.330(1)	78.284(1)
V/Å^3	1348.8(2)	1174.4(1)
Z	1	1
μ/mm^{-1}	0.990	1.127
GOF on F^2	1.053	1.045
fianl R indices $[I > 2\sigma(I)]^a$	R1 = 0.0472, wR2 = 0.1220	R1 = 0.0358, wR2 = 0.0790
R indices (all data)^a	R1 = 0.0782, wR2 = 0.1354	R1 = 0.0585, wR2 = 0.0884

^{a} $R1 = \sum F_o| - |F_c/\sum|F_o|$. $wR2 = \sum w(F_o^2 - F_c^2)^2/\sum wF_o^2)^{1/2}$.

Scheme 1

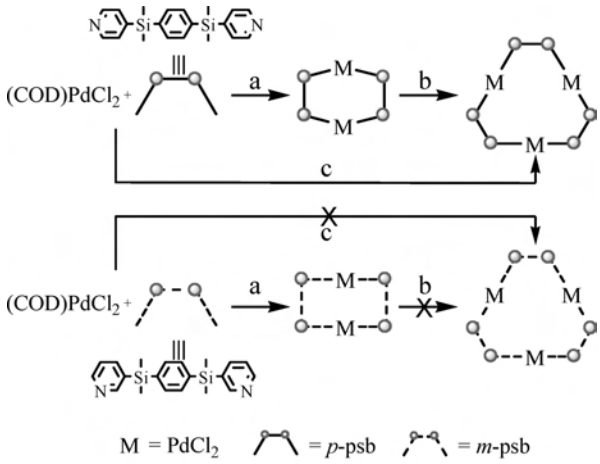

(a) reaction at room temperature (b) sonication or reflux (c) reaction at reflux condition

thermal factors. The crystal parameters and procedural information corresponding to the data collection and structure refinement are listed in Table 1.

Results and Discussion

Synthesis. The reaction of $(COD)PdCl_2$ with a *p*- or *m*-psb ligand in a mixture of acetone and ethanol at room temperature yields discrete cyclodimers of $[PdCl_2(p\text{- or } m\text{-psb})]_2$ in high yield, as shown in Scheme 1. However, the reaction of $(COD)PdCl_2$ with *p*-psb at reflux temperature gives only a cyclotrimeric species of $[PdCl_2(p\text{-psb})]_3$, whereas the reaction of $(COD)PdCl_2$ with *m*-psb even at reflux temperature yields the cyclodimer. Furthermore, $[PdCl_2(p\text{-psb})]_2$ at boiling temperature or via sonication of chloroform solution is exclusively converted to the cyclotrimer, whereas $[PdCl_2(m\text{-psb})]_2$ is retained, even under the same treatment conditions. Equilibrium between $[PdCl_2(p\text{-psb})]_2$ and $[PdCl_2(p\text{-psb})]_3$ in *N*,*N*-dimethylformamide or dimethyl sulfoxide was observed, as will be explained in detail. The reactions were originally conducted in the 1:1 mol ratio of palladium(II) to psb ligand, but the products were not significantly affected by either the mole ratio or the concentrations. The present products are remarkable in that there was no evidence for polymerization, not even under the high concentrations and despite the lack of protective groups. The formation of discrete cyclomolecules can be attributed to the horse-shoe psb ligands. Thin yellow crystalline products of $[PdCl_2(p\text{- or } m\text{-psb})]_2$ are soluble in dichloromethane, chloroform, *N*,*N*-dimethylformamide, and dimethyl sulfoxide but are insoluble in water, hexane, ethanol, nitromethane, and acetone. $[PdCl_2(p\text{-psb})]_3$ is slightly soluble in dichloromethane. The results of an elemental analysis and the NMR spectra of the products were consistent with the desirable structures.

Crystal Structures of $[PdCl_2(p\text{-psb})]_2$ and $[PdCl_2(m\text{-psb})]_2$. The crystal structures of $[PdCl_2(p\text{-psb})]_2$ and $[PdCl_2(m\text{-psb})]_2$ are depicted in Figure 1, and the relevant bond lengths and angles are listed in Table 2. For both compounds, the local geometry around the palladium(II) approximates to a typical square-planar arrangement with two chlorides in the trans position (Cl1−Pd−Cl2 = 175.86(5)° for $[PdCl_2(p\text{-psb})]_2$ and 177.75(4)° for $[PdCl_2(m\text{-psb})]_2$). The neutral psb ligand connects two palladium(II) ions to form a 30-membered cyclodimer for $[PdCl_2(p\text{-psb})]_2$ and a 26-membered cyclodimer for $[PdCl_2(m\text{-psb})]_2$. The *p*- and *m*-psb ligands act as the unusual horse-shoe units, which are useful for the construction of molecular rectangles.[28] The structures of both cyclodimer compounds are basically similar, but their bond strengths and angles around the palladium(II) are slightly different, presumably owing to the different ring constraints between the two compounds. The environment around the palladium(II) is very sensitive to the N position of the psb ligands. That is, the Pd−Cl [2.305(2) and 2.307(1) Å] and Pd–N [2.012(5) and 2.027(5) Å] lengths of $[PdCl_2(p\text{-psb})]_2$ are slightly longer than those [2.301(1) and 2.303(1) Å; 2.009(3) and 2.016(3) Å] of $[PdCl_2(m\text{-psb})]_2$. The N–Pd–N [176.4(2)°] and Cl−Pd−Cl [175.86(5)°] angles of $[PdCl_2(p\text{-psb})]_2$ are more deviated from an ideal linear angle than those [179.0(1)°; 177.75(4)°] of $[PdCl_2(m\text{-psb})]_2$. Thus, there is the significant difference in the bond lengths and ring constraints between the two compounds in the solid state. For $[PdCl_2(m\text{-psb})]_2$, the intracyclic Pd···Pd distance (8.53 Å) is very similar to the intraligand N1···N2 distance (8.52 Å), whereas for $[PdCl_2(p\text{-psb})]_2$, the intracyclic Pd···Pd distance (8.52 Å) is longer than the intraligand N1···N2 distance (8.39 Å). Such a fact indicates that the ring constraints of $[PdCl_2(p\text{-psb})]_2$ are larger than those of $[PdCl_2(m\text{-psb})]_2$. Both cyclodimeric

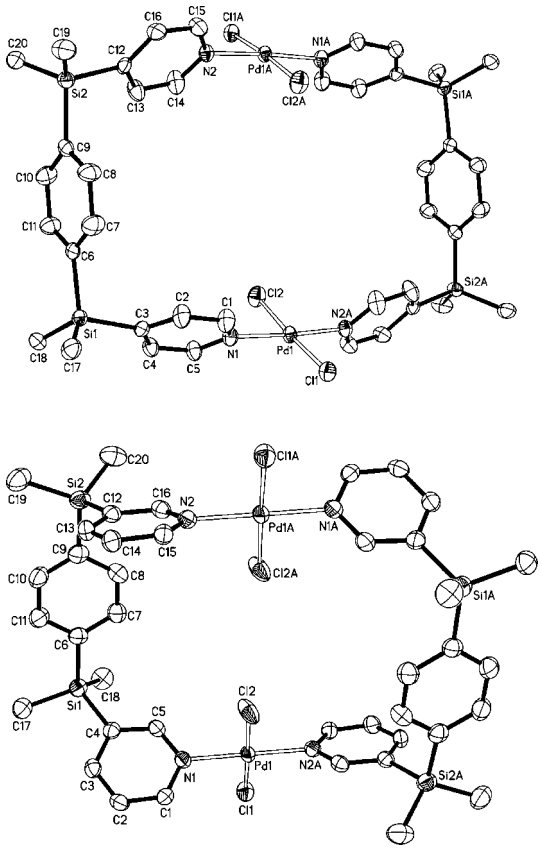

Figure 1. ORTEP views of $[PdCl_2(p\text{-psb})]_2$ (top) and $[PdCl_2(m\text{-psb})]_2$ (bottom). All hydrogen atoms and solvate ethanol molecules are omitted for clarity.

Table 2. Relevant Bond Lengths (Å) and Angles (deg) for $[PdCl_2(p\text{-psb})]_2$ and $[PdCl_2(m\text{-psb})]_2$

$[PdCl_2(p\text{-psb})]_2$		$[PdCl_2(m\text{-psb})]_2$	
Pd1−N1	2.027(4)	Pd1−N1	2.009(3)
Pd1−N2′	2.013(4)	Pd1−N2′	2.016(3)
Pd1−Cl1	2.307(1)	Pd1−Cl1	2.303(1)
Pd1−Cl2	2.305(2)	Pd1−Cl2	2.301(1)
N1−Pd1−N2′	176.4(2)	N1−Pd1−N2′	179.0(1)
Cl1−Pd1−Cl2	175.86(5)	Cl1−Pd1−Cl2	177.75(4)
N1−Pd1−Cl1	90.7(1)	N1−Pd1−Cl1	89.07(9)
N1−Pd1−Cl2	89.8(1)	N1−Pd1−Cl2	89.66(9)
N2′−Pd1−Cl1	91.4(1)	N2′−Pd1−Cl1	91.61(9)
N2′−Pd1−Cl2	88.0(1)	N2′−Pd1−Cl2	89.69(9)
C3−Si1−C6	107.3(2)	C4−Si1−C6	111.2(2)
C3−Si1−C17	108.2(3)	C4−Si1−C17	107.6(2)
C3−Si1−C18	108.9(2)	C4−Si1−C18	106.9(2)
C6−Si1−C17	110.2(2)	C6−Si1−C17	109.4(2)
C6−Si1−C18	109.8(2)	C6−Si1−C18	108.9(2)
C17−Si1−C18	112.3(3)	C17−Si1−C18	112.8(2)
C9−Si2−C12	105.2(2)	C9−Si2−C12	106.7(2)
C9−Si2−C19	110.7(2)	C9−Si2−C19	109.3(2)
C9−Si2−C20	109.7(2)	C9−Si2−C20	110.8(2)
C12−Si2−C19	109.4(3)	C12−Si2−C19	108.6(2)
C12−Si2−C20	109.6(2)	C12−Si2−C20	109.1(2)
C19−Si2−C20	112.1(3)	C19−Si2−C20	112.1(2)

products are discrete molecules with no close intermolecular contacts. No other exceptional features, including those of either bond lengths or angles, were observed.

^{1}H NMR Behavior in Solution. The ^{1}H NMR spectra of $[PdCl_2(p\text{-psb})]_2$ and $[PdCl_2(m\text{-psb})]_2$ in chloroform at room temperature are consistent with the crystal structures. $[PdCl_2(p\text{-psb})]_2$ is unusually nonrigid in solution under relatively vigorous conditions. After $[PdCl_2(p\text{-psb})]_2$ was sonicated in chloroform, the signals of the *p*-pyridyl group exhibited two sets of ^{1}H NMR resonances (7.19 and 8.64 ppm; 7.37 and 8.71 ppm), confirming the coexistence of the two species in the solution. In the initial state, the signals at 7.19 and 8.64 ppm were predominant, and finally the original signals were completely replaced by the signals at 7.37 and 8.71 ppm with similar splitting patterns. The phenyl peak at 7.50 ppm was shifted to 7.46 ppm, as shown in Figure 2, indicating that $[PdCl_2(p\text{-psb})]_2$ in chloroform was transformed into a new species. The new transformed product could be isolated and characterized by elemental analysis, thermogravimetric analysis (TGA), differential scanning calorimetry (DSC), IR, ^{1}H NMR, and MS data. All of the data of the transformed compound are very similar to those of the original cyclodimer except for the MS data. The MS data of $[PdCl_2(p\text{-psb})]_2$, $[PdCl_2(m\text{-psb})]_2$, and the new species were obtained to characterize the new species (Figure 3). As expected, the similar MS data of $[PdCl_2(p\text{-psb})]_2$ and $[PdCl_2(m\text{-psb})]_2$ [*m/e* 1017.6 $[M - Cl]^+$ (calcd *m/e* 1017.0)] indicated the dimeric products. In contrast, the main mass peaks of the new species [*m/e* 1541.4 $[M - Cl]^+$ (calcd *m/e* 1541), 1193.6 $[M - Cl - L]^+$ calcd *m/e* 1193), 1157.7 $[M - L - Cl - HCl]^+$ (calcd *m/e* 1157), 1018.0 $[M - PdCl_2 - L - Cl]^+$ (calcd *m/e* 1018.0)] clearly indicate that the new transformed species is a cyclotrimer of $[PdCl_2(p\text{-psb})]_3$. The cyclotrimeric product was obtained in crystal form, but its crystal structure was not solved, owing to severely solvated chloroform molecules as well as a very thin crystalline state. Of course, the ^{1}H NMR spectrum indicates that the product prepared from the direct reaction at reflux temperature is the same cyclotrimer. An interesting feature is that the peak ratio of the pyridyl protons is dependent on the polarity of the solvents. The structures of $[PdCl_2(p\text{-psb})]_2$ and $[PdCl_2(p\text{-psb})]_3$ were retained in chloroform without any sonication at room tem-

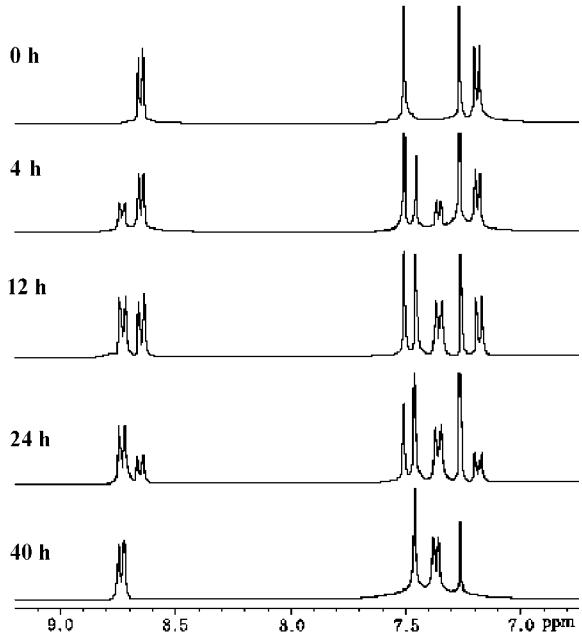

Figure 2. ^{1}H NMR spectra on a conversion process of $[PdCl_2(p\text{-psb})]_2$ to $[PdCl_2(p\text{-psb})]_3$ in $CDCl_3$ via sonication.

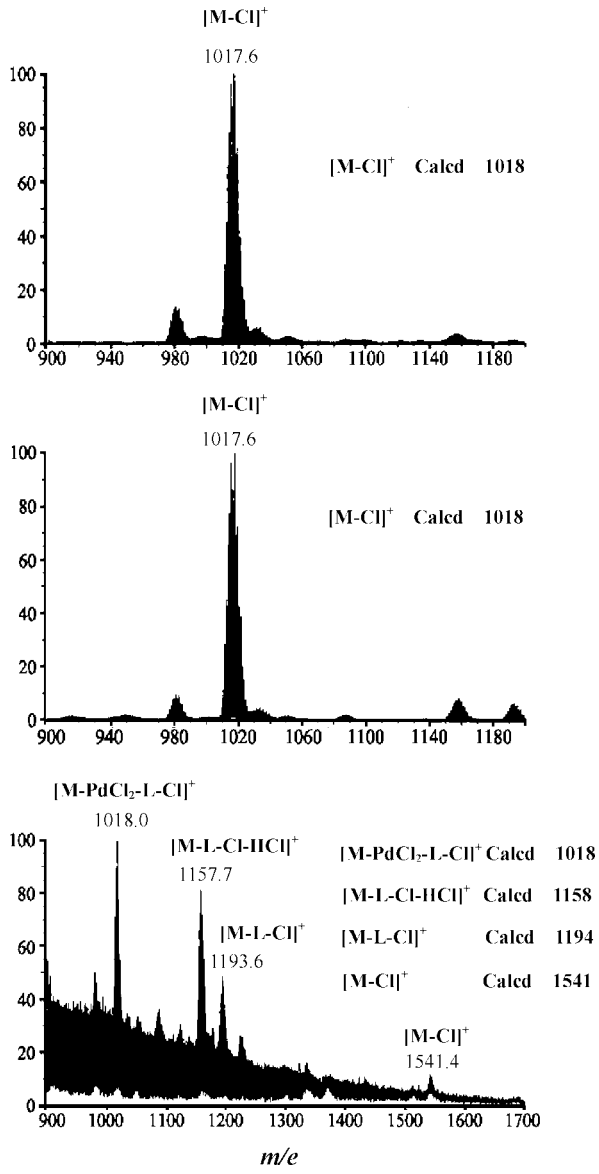

Figure 3. FAB-MS data of $[PdCl_2(m\text{-psb})]_2$ (a), $[PdCl_2(p\text{-psb})]_2$ (b), and $[PdCl_2(p\text{-psb})]_3$ (c).

perature, but the equilibrium between $[PdCl_2(p\text{-psb})]_2$ and $[PdCl_2(p\text{-psb})]_3$ existed in *N*,*N*-dimethylformamide at room temperature. At the initial stage, $[PdCl_2(p\text{-psb})]_2$ in the solution was in the mole ratio of 92:8 and finally arrived at the mole ratio equilibrium of 48:52 after 12 h (Figure 4a). Similarly, $[PdCl_2(p\text{-psb})]_3$ in *N*,*N*-dimethylformamide initially existed as a mixture of $[PdCl_2(p\text{-psb})]_2$ and $[PdCl_2(p\text{-psb})]_3$ in 5:95 and finally reached the equilibrium of 42:58 (Figure 4b). $[PdCl_2(p\text{-psb})]_2$ in dimethyl sulfoxide existed as a mixture of $[PdCl_2(p\text{-psb})]_2$ and $[PdCl_2(p\text{-psb})]_3$ in the mole ratio of 30:70. $[PdCl_2(p\text{-psb})]_3$ behaved similarly in the solution (Supporting Information). As time passed, the Me_2SO solution produced another set of peaks, presumably owing to the genesis of the dimethyl sulfoxide-coordinated species. The ratios of $[PdCl_2(p\text{-psb})]_2$ and $[PdCl_2(p\text{-psb})]_3$ in each solvent are listed in Table 3. In contrast, $[PdCl_2(m\text{-psb})]_2$, under the same treatment, is rigid in solution for 40 h.

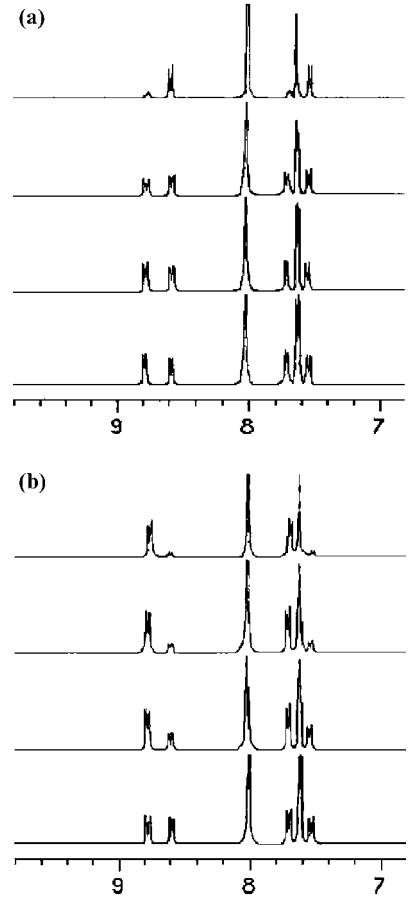

Figure 4. ^1H NMR spectra on a conversion of $[PdCl_2(p\text{-psb})]_2$ to $[PdCl_2(p\text{-psb})]_3$ (a) and a conversion of $[PdCl_2(p\text{-psb})]_3$ to $[PdCl_2(p\text{-psb})]_2$ (b) in *N*,*N*-dimethylformamide-d_7 via sonication.

Table 3. Ratios of $[PdCl_2(p\text{-psb})]_2 \rightleftarrows [PdCl_2(p\text{-psb})]_3$ in Each Solvent via Sonication

	d:t[a] for $[PdCl_2(p\text{-psb})]_2$ ($[PdCl_2(p\text{-psb})]_3$)		
	$CHCl_3$	$Me_2N(CO)H$	Me_2SO
0 h	100:0 (0:100)[b]	92:8 (5:95)	30:70 (30:70)
4 h	70:30 (−)	54:46 (12:88)	
8 h	57:42 (−)	48:52 (20:80)	
12 h	49:51 (−)	− (29:71)	
24 h	29:71 (−)	− (35:65)	
40 h	0:100 (−)	− (42:58)	

[a] d: $[PdCl_2(p\text{-psb})]_2$. t: $[PdCl_2(p\text{-psb})]_3$. [b] Parentheses values are the ratio of $[PdCl_2(p\text{-psb})]_2/[PdCl_2(p\text{-psb})]_3$ by sonication of $[PdCl_2(p\text{-psb})]_3$.

The present ring expansion of $[PdCl_2(p\text{-psb})]_2$ seems to be attributable to the transformation of the kinetic product, $[PdCl_2(p\text{-psb})]_2$, to the thermodynamic product, $[PdCl_2(p\text{-psb})]_3$. This ring expansion results from the ring constraint of the cyclodimer $[PdCl_2(p\text{-psb})]_2$. This ring constraint decreases the Pd−N bond strength relative to $[PdCl_2(m\text{-psb})]_2$, as discussed with regard to the crystal structures. Moreover, another important factor in the ring expansion was the polarity of the solvent. Thus, the driving force behind the present ring expansion can be ascribed to a suitable combination of media and ring constraint.

Thermal Analysis. The TGA and DSC curves of $[PdCl_2(p\text{-psb})]_2$ and $[PdCl_2(p\text{-psb})]_3$ are depicted in Figure 5. Their thermal analyses were carried out after evaporation of the solvate ethanol and chloroform molecules. Their TGA curves are very similar, indicating that the skeletal structures are

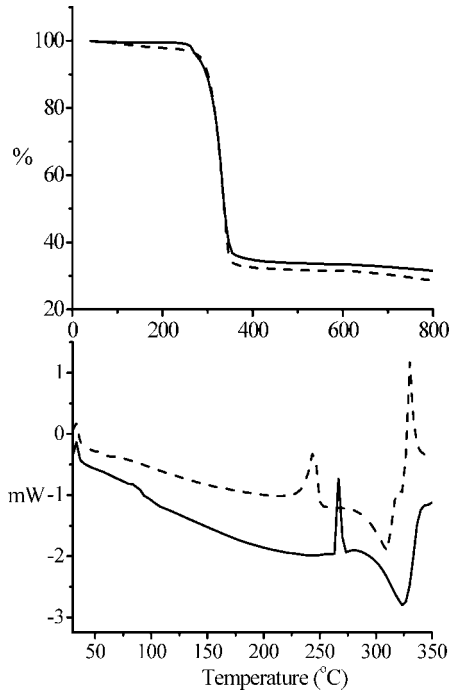

Figure 5. TGA (top) and DSC (bottom) curves of $[PdCl_2(p\text{-psb})]_2$ (solid line) and $[PdCl_2(p\text{-psb})]_3$ (dashed line).

similar as well as thermally stable up to 300 °C. As shown, a drastic loss of mass corresponding to *p*-psb was observed (obsd 60–64.0%; calcd 66.3%). The DSC curves indicate that the melting points of $[PdCl_2(p\text{-psb})]_2$ and $[PdCl_2(p\text{-psb})]_3$ are 270 and 240 °C, respectively, owing presumably to the difference of the crystal-lattice energy.

Reaction of $[PdCl_2(p\text{-psb})]_2$ with Amine. Treatment of $[PdCl_2(p\text{-psb})]_2$ with triethylamine easily trimerizes to $[PdCl_2(p\text{-psb})]_3$. The same treatment of $[PdCl_2(p\text{-psb})]_2$ with triethanolamine instead of triethylamine produces a trimeric substituent. In particular, the addition of triethanolamine into the NMR solution of $[PdCl_2(p\text{-psb})]_3$ suggests the formation of $[Pd(OCH_2CH_2N(OCH_2CH_2OH)_2)_2(p\text{-psb})]_3$. However, the substituent trimer could not be clearly isolated owing to its sticky properties. During the reaction in the NMR tube, of course, quaternary ammonium salts of triethanolamine·HCl were isolated and characterized. These results indicate that

Scheme 2

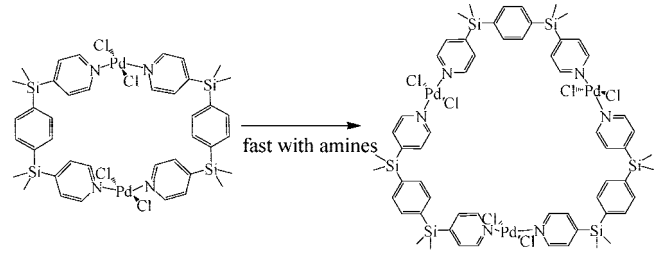

triethylamine as a base catalyst accelerates the ring expansion without additional agitation or energy. That is, amine catalyzes to dissociate the Pd−N bond of $[PdCl_2(p\text{-psb})]_2$ and accelerates to form the thermodynamically stable cyclotrimer and substituent without any sonication or reflux heat, as depicted in Scheme 2. As expected, when $[PdCl_2(p\text{-psb})]_2$ was treated with ethylene glycol, the trimerization and the substitution reaction of ethylene glycol did not take place.

Conclusion

The present discrete metallacyclic compounds demonstrate that the psb ligands are unique horse-shoe ligands. The ring-expansion route to $[PdCl_2(p\text{-psb})]_3$ can be induced from a combination of ring constraint and solvents. This presents a synthetic strategy for obtaining successive ring control in metallacyclic compounds. Indeed, this unusual process can contribute to the desirable molecular cyclic materials applicable to sensor technology, transport, catalysis, and molecular switching. Further experiments aimed at clarifying the mechanistic aspects are in progress.

Acknowledgment. This work is supported by the KRF-2006-312-C00578 in Korea.

Supporting Information Available: Crystallographic data for $[PdCl_2(p\text{-psb})]_2$ and $[PdCl_2(m\text{-psb})]_2$ in CIF format, IR spectra of $[PdCl_2(p\text{-psb})]_2$ and $[PdCl_2(p\text{-psb})]_3$, ^1H NMR of $[PdCl_2(p\text{-psb})]_2$ and $[PdCl_2(p\text{-psb})]_3$ in $Me_2SO\text{-}d_6$, ^1H NMR of $[Pd(OCH_2CH_2N(OCH_2CH_2OH)_2)_2(p\text{-psb})]_3$, ^1H NMR of $[PdCl_2(p\text{-psb})]_2$ with triethylamine, a photograph of crystalline $[PdCl_2(p\text{-psb})]_3$. This material is available free of charge via the Internet at http://pubs.acs.org.

IC701489P